Available online at www.sciencedirect.com
ScienceDirect
Earth and Planetary Science Letters 263 (2007) 207–220
EPSL
www.elsevier.com/locate/epsl

Regional-scale climate influences on temporal variations of rainwater and cave dripwater oxygen isotopes in northern Borneo

Kim M. Cobb [a,*], Jess F. Adkins [b], Judson W. Partin [a], Brian Clark [c]

[a] School of Earth and Atmospheric Sciences, Georgia Inst. of Technology, 311 Ferst Dr., Atlanta, GA 30332, United States
[b] Department of Geological and Planetary Sciences, California Inst. of Technology, Pasadena, CA 91125, United States
[c] Gunung Mulu National Park, Sarawak, Malaysia

Received 23 February 2007; received in revised form 22 August 2007; accepted 22 August 2007
Available online 31 August 2007
Editor: M.L. Delaney

Abstract

This study investigates the relationship between large-scale climate variability, rainfall oxygen isotopic composition ($\delta^{18}O$), and cave dripwater $\delta^{18}O$ at Gunung Mulu and Gunung Buda National Parks in northern Borneo (4°N, 115°E) on intraseasonal to interannual timescales. A 3-yr timeseries of rainfall $\delta^{18}O$ contains prominent seasonal and interannual variability. The seasonal cycle in rainfall $\delta^{18}O$ is defined by lighter values of − 10‰ during late boreal summer and heavier values of − 4‰ during late boreal winter, and is poorly correlated to local precipitation, which displays very weak seasonality. Seasonally-varying moisture trajectories likely play a key role in the observed seasonal cycle of rainfall $\delta^{18}O$, driving enhanced fractionation during boreal summer and less fractionation during boreal winter. Dripwater $\delta^{18}O$ timeseries display 2‰ seasonal cycles that follow the rainfall $\delta^{18}O$ seasonal cycles, with a mean $\delta^{18}O$ value equivalent to the mean $\delta^{18}O$ of rainfall. Large surveys of cave dripwaters conducted during three fieldtrips to Gunung Mulu/Buda reveal a system-wide response to rainfall $\delta^{18}O$ seasonality that supports a relatively short (less than 6months) response time for most drips. During the weak 2005/2006 La Niña event, sustained positive precipitation anomalies are associated with rainfall $\delta^{18}O$ values that are 4 to 5‰ lighter than previous years' values, consistent with the tropical "amount effect" observed in both models and data. Dripwater $\delta^{18}O$ values are 1 to 2‰ lighter during the weak La Niña event. The importance of the "amount effect" in driving intraseasonal rainfall $\delta^{18}O$ anomalies at our site is supported by an 8‰ increase in rainfall $\delta^{18}O$ that occurred over the course of two weeks in response to a pronounced decrease in regional convective activity. Dripwater discharge rates underwent a ten-fold decrease during the extended dry period, but dripwater $\delta^{18}O$ values remained constant. This study supports the interpretation of stalagmite $\delta^{18}O$ records from Gunung Mulu/Buda as paleo-precipitation records that are sensitive to the location and strength of deep convection in the West Pacific Warm Pool.

Keywords: stalagmite; rainfall; dripwater; oxygen isotopes; paleoclimate; West Pacific Warm Pool

1. Introduction

Stalagmite oxygen isotopic records have provided long, high-resolution, absolutely-dated climate reconstructions from many regions of the globe. Such reconstructions have played a particularly important role

* Corresponding author. Tel.: +1 404 894 1992; fax: +1 404 894 5638.
E-mail address: kcobb@eas.gatech.edu (K.M. Cobb).

0012-821X/$ - see front matter © 2007 Elsevier B.V. All rights reserved.
doi:10.1016/j.epsl.2007.08.024

in the tropics, where high-resolution, absolutely-dated paleoclimate archives are scarce. Indeed, tropical stalagmite oxygen isotopic ($\delta^{18}O$) records conclusively link precipitation variability in southeastern Asia (Wang et al., 2001), the Arabian Sea (Burns et al., 2003), and the eastern Mediterranean (Bar-Matthews et al., 1999) to abrupt climate change events recorded in the Greenland ice cores (Grootes et al., 1993). Millennial-scale variability in stalagmite $\delta^{18}O$ records points to precessional forcing as the dominant control on orbital-scale tropical hydrology (Fleitmann et al., 2003; Yuan et al., 2004; Cruz et al., 2005a,b; Dykoski et al., 2005; Cruz et al., 2006; Wang et al., 2006; Partin et al., 2007), while centennial-scale variability in stalagmite $\delta^{18}O$ records that span the last millennium document tropical hydrological effects associated with the 'Medieval Warm Period' and the 'Little Ice Age' (Burns et al., 2002; Fleitmann et al., 2004; Lachniet et al., 2004).

Despite the increasingly important role that stalagmite $\delta^{18}O$ records play in global climate change studies, their interpretation with respect to large-scale climate dynamics is often ambiguous. In the tropics, stalagmite $\delta^{18}O$ records are largely interpreted as rainfall $\delta^{18}O$ reconstructions, with a minor role for relatively small temperature changes that occur in the tropics. Potential controls on rainfall $\delta^{18}O$ variability include temperature-dependent changes in the vapor-liquid fractionation factor, changes in the water vapor source region, and the cumulative effect of Raleigh fractionation that occurs as vapor condensation proceeds (Dansgaard, 1964; Rozanski et al., 1993; Gat, 1996). An empirical relationship referred to as the 'amount effect' exists between rainfall $\delta^{18}O$ and rainfall amount in the tropics, and likely arises from more extensive rainout (and therefore larger rainfall $\delta^{18}O$ depletions) and/or less evaporative enrichment of raindrops during wet periods. On regional scales, atmospheric general circulation models equipped with stable isotope tracers have reproduced the strong inverse relationship between the amount of precipitation and the $\delta^{18}O$ of rainfall throughout the tropics (Jouzel et al., 1987; Hoffmann et al., 1998; Cole et al., 1999; Noone and Simmonds, 2002; Vuille et al., 2005; Brown et al., 2006). However, both models and data highlight the importance of variable moisture sources and trajectories in contributing to significant seasonal and interannual rainfall $\delta^{18}O$ variability in the tropics, especially in regions characterized by monsoonal circulation and/or proximity to large-scale atmospheric fronts (Araguas-Araguas et al., 1998; Cole et al., 1999; Cruz et al., 2005a,b; Vuille and Werner, 2005; Vuille et al., 2005). Detailed on-site analyses of the relationship between large-scale climate and local rainfall $\delta^{18}O$ are critical to accurate climatic interpretations of many terrestrial paleoclimate reconstructions based on ice core, tree ring, or stalagmite $\delta^{18}O$, but few such studies exist.

Even if the climate-rainfall $\delta^{18}O$ relationship is well-constrained, cave hydrology adds an additional layer of complexity to the interpretation of stalagmite $\delta^{18}O$ records. The climate-related rainfall $\delta^{18}O$ signal must be transmitted through the dynamic karst system, which involves mixing in the epikarst, possible evaporative fractionation, and highly variable groundwater flow rates. Dripwater residence times vary from several months in tropical regions (Cruz et al., 2005a,b; Johnson et al., 2006) to decades in semi-arid regions (Ayalon et al., 1998), depending on the recharge and mixing characteristics of a given cave system. Prolonged rainfall anomalies can cause temporal variability in dripwater residence times (McDonald et al., 2004), while different dripwater pathways contribute to spatial heterogeneity in residence times (Ayalon et al., 1998). Quantitative calibrations of high-resolution stalagmite $\delta^{18}O$ records to the instrumental climate record (e.g. Fleitmann et al., 2004; Treble et al., 2005b) provide the most direct measure of climatic influences on stalagmite $\delta^{18}O$, but such calibrations are exceedingly rare and may be impossible to undertake at some sites. Therefore, detailed site-specific investigations of the relationship between large-scale climate, rainfall $\delta^{18}O$ variability, cave hydrology, and dripwater $\delta^{18}O$ variability are critical to accurate interpretations of stalagmite $\delta^{18}O$ variability.

In this study we investigate the large-scale climatic controls on rainfall and dripwater $\delta^{18}O$ variability in northern Borneo, where climate is dominated by monsoonal variability and the El Niño-Southern Oscillation. As no GNIP (http://isohis.iaea.org) rainfall $\delta^{18}O$ data exist from Borneo, this study is key to accurate interpretations of several new stalagmite $\delta^{18}O$ reconstructions that extend through the Last Glacial Maximum from the site (Partin et al., 2007). A 3-yr-long on-site rainfall and dripwater monitoring program is supplemented with intensive sampling during three fieldtrips in 2003, 2005, and 2006 to provide constraints on both spatial and temporal variability in rainwater and dripwater $\delta^{18}O$. The resulting $\delta^{18}O$ timeseries are compared against local rainfall as well as gridded datasets of precipitation and wind in an attempt to isolate the climatic controls on rainfall and dripwater $\delta^{18}O$ across synoptic, seasonal, and interannual timescales.

2. Geologic setting

The research site is located in the adjoining Gunung Mulu and Gunung Buda National Parks (4°N, 115°E), in

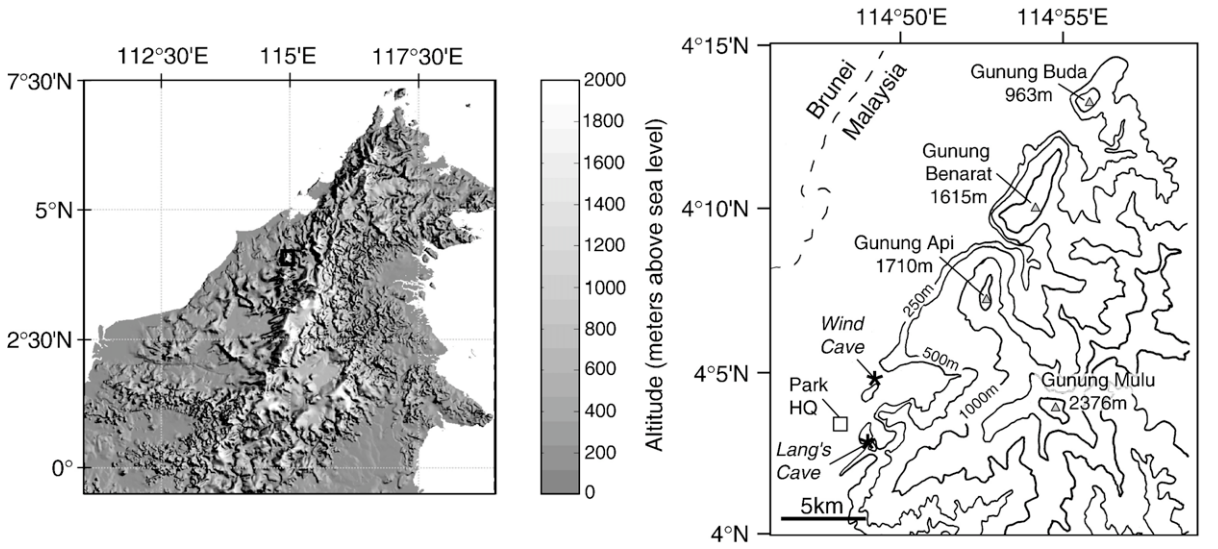

Fig. 1. (left) Topographic map of Borneo (GTOPO30 data, available at http://eros.usgs.gov/). Note that the scale was chosen to maximize contrast at low elevations, meaning that peaks above 2000 m a.s.l. are saturated. Thick black box represents inset map. (right) Topographic map of Gunung Mulu National Park, Sarawak, Malaysia, showing locations of research caves (after Fig. 86 of Hazebroeck and Morshidi, 2002).

northern Sarawak, Malaysian Borneo (Fig. 1). The caves formed in the northeast-striking Melinau limestone formation, driven by runoff flowing down the northwestern flank of Gunung Mulu peak, a sandstone formation which rises to an elevation of 2376m above sea level (Fig. 1). Rivers have cut steep gorges through the Melinau limestone to form topographically isolated mounds of carbonate which rise from the base of the rainforest (~ 100m above sea level) to 1710m above sea level, in the case of Gunung Api, the largest of the Melinau carbonate mounds. Therefore, these active karst systems are presently fed exclusively by rainfall that falls directly over the carbonate mounds. Gunung Mulu National Park, a UNESCO world heritage site, contains all of the Melinau carbonate mounds with the exception of Gunung Buda, which is contained within a separate, undeveloped national park to the north of Gunung Mulu. A September, 2003 expedition included collections from Snail Shell, Mojo, Chin Chin, Green Cathedral, and Bukit Assam caves, all located within Gunung Buda. Expeditions during March, 2005 and June, 2006 expeditions included return visits to Snail Shell and Mojo caves at Gunung Buda, as well as Lang's, Wind, Clearwater, and Deer caves at Gunung Mulu. Detailed information concerning overburden, distance from cave entrances, and soil cover is not available for these remote cave systems. In situ logging devices measured stable relative humidity levels of ~ 100% in the caves.

3. Climatic setting

Warm sea-surface temperatures drive year-round atmospheric deep convection in northern Borneo, which receives over 5m of rainfall per year with weak seasonality (Fig. 2), as documented by daily precipitation data collected at the Mulu airport since 1998. Analysis of the Mulu airport rainfall data reveals that intraseasonal (30–60day) variability (Madden and Julian, 1971; Madden and Julian, 1972; Knutson and Weickmann, 1987) accounts for approximately 20% of total precipitation variance at the research site, roughly equivalent to the variance contribution from weak seasonal variability. Temperatures lie between 26 and 27°C year-round, as recorded by on-site temperature loggers.

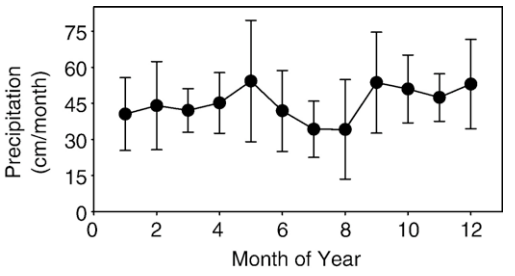

Fig. 2. Seasonal precipitation cycle for Mulu airport (shown with 1σ s.d.), calculated from June 1998 to December 2005.

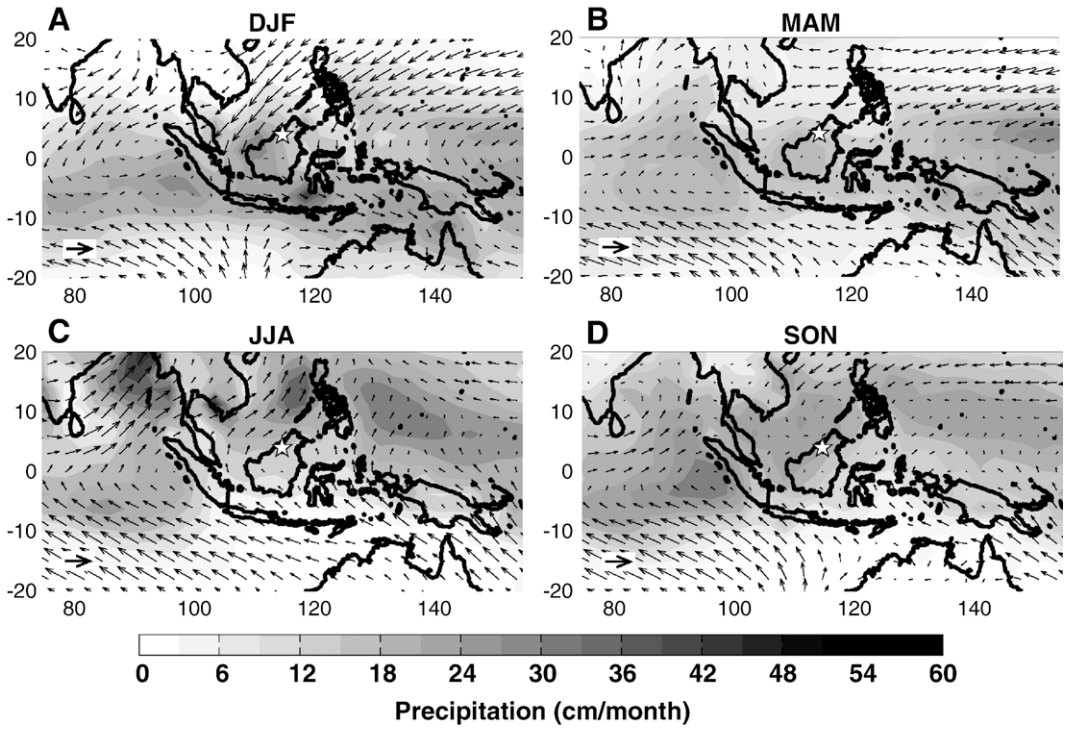

Fig. 3. Precipitation (shaded) and 1000 mb wind (arrows) climatology maps for the Western Pacific. (A) Mean precipitation and winds for December through February (DJF). A 5 m/s wind vector (shown in white box) is plotted for reference. (B) Same as (A) but for March through May (MAM). (C) Same as (A) but for June through August (JJA). (D) Same as (A) but for September through November (SON). CMAP precipitation (Xie and Arkin, 1997) and NCEP wind data (Kalnay et al., 1996) provided by the NOAA/OAR/ESRL PSD, Boulder, Colorado, USA, from their web-site at http://www.cdc.noaa.gov/.

Maps of precipitation in the Western tropical Pacific confirm that the precipitation maximum associated with the Intertropical Convergence Zone (ITCZ) does not leave northern Borneo in its meridional migration (Fig. 3), explaining the weak seasonality observed in the local Mulu rainfall data. Small precipitation maxima are observed in boreal fall and in late boreal spring (Fig. 2), when large-scale meridional temperature gradients are at a minimum. Prevailing wind direction displays marked seasonality, however, with more northerly winds occurring during boreal winter, while southerly winds occur during boreal summer (see also Figs. 1 and 2 of Lau and Nath, 2000).

The largest changes in Warm Pool convective activity occur during extremes of the El Niño-Southern Oscillation (ENSO). During El Niño events, warm sea-surface temperatures (SSTs) in the central to eastern Pacific drive an eastward shift in convection (Rasmusson and Wallace, 1983), leading to drought in northern Borneo that begins in boreal fall and persists through boreal spring (Ropelewski and Halpert, 1987; Lau and Nath, 2003). Indeed, boreal winter precipitation in northern Borneo was reduced by more than 50% during the 1997/1998 El Niño event. Convection strengthens over the Warm Pool during La Niña events. Precipitation in northern Borneo is highly correlated to the Southern Oscillation Index (SOI) (Fig. 4), an index which tracks the seesaw in atmospheric pressure that occurs during ENSO extremes. Maps of the SOI regressed against seasonal precipitation and wind data confirm the year-round impact of ENSO on northern

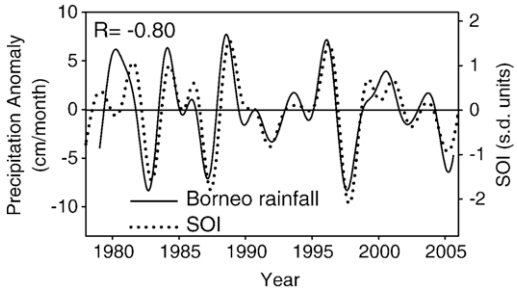

Fig. 4. Interannual variability of northern Borneo precipitation (grid-point centered at 3.75°N, 113.75°E, CMAP data) (Xie and Arkin, 1997) plotted with the Southern Oscillation Index (http://www.cpc.noaa.gov/data/indices/). Both timeseries have been filtered with a 2–7 yr bandpass filter.

Borneo precipitation (Fig. 5). Seasonal wind anomalies in northern Borneo have a slight easterly (westerly) tendency during El Niño (La Niña) events, but the effect is not statistically significant.

The geographic and climatic setting of our research site means that there are several potential mechanisms for the fractionation of rainfall oxygen isotopes. First, the presence of large mountains to the east of the site means that orographic fractionation may occur (Dansgaard, 1964; Siegenthaler and Oeschger, 1980), whereby large isotopic depletions are driven by both enhanced rainout and cooler fractionation temperatures as an air parcel moves across a mountain range. Second, varying moisture trajectories could lead to fractionation via enhanced rainout, referring to the progressive Raleigh-type distillation that occurs as isotopically enriched rain falls from an air parcel. This latter effect is analogous to the "continental effect" or "degree of rainout"

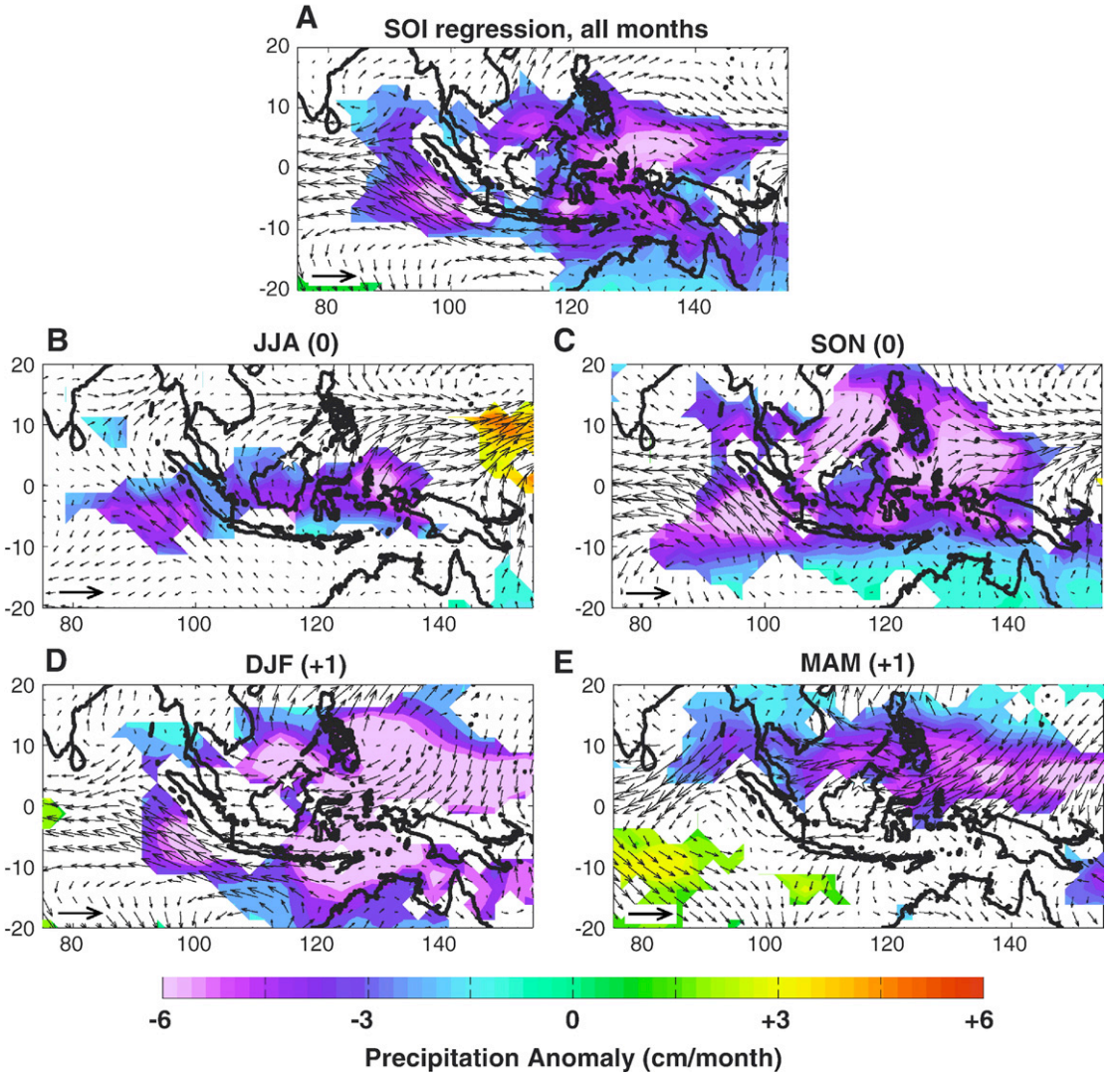

Fig. 5. Regression maps for the Southern Oscillation Index (SOI) and western Pacific precipitation and wind anomalies. (A) Map of monthly precipitation and wind anomalies regressed on the SOI, showing that negative SOI (an El Niño event) is strongly correlated to decreased rainfall over the western Pacific. Only precipitation anomaly correlations above 95% are plotted (significance assessed with a student's *t*-test using reduced degrees of freedom to account for auto-correlation). Wind anomaly correlations are not significant above the 95% level, but are plotted nonetheless. A 5 m/s wind vector (shown in white box) is plotted for reference. (B) Same as (A), but JJA precipitation and wind anomalies for the boreal summer season preceding peak ENSO anomalies are regressed onto peak (DJF) SOI anomalies. (C) Same as (B) but for SON precipitation and wind anomalies (i.e. during fall preceding peak ENSO anomalies). (D) Same as (C) but for DJF precipitation and wind anomalies (i.e. during peak ENSO anomalies). (E) Same as (D) but for MAM precipitation and wind anomalies (i.e. during spring following peak ENSO anomalies).

mentioned in previous studies (Rozanski et al., 1993; Vuille and Werner, 2005). Lastly, fractionation may occur through a more local "amount effect", driven by evaporation and condensation in organized deep convection closer to the site.

4. Methods

Two distinct sets of rainfall samples were collected at Gunung Mulu/Buda — one set for the 3-yr continuous monitoring program, and another set that represents samples collected during fieldtrips. The continuous rainfall $\delta^{18}O$ timeseries is constructed from two-week cumulative rainfall samples collected in an oil-type, foil-covered reservoir following standard water isotope collection protocols (Friedman et al., 1992). Bi-weekly, cumulative rainwater sampling was conducted during isolated intervals at nearby Long Napir (4°10′N, 115°8′E) and Gunung Buda, and quasi-continuously at Gunung Mulu from October 2003 to July 2006. Rainfall $\delta^{18}O$ samples taken during fieldtrips represent snapshots of single rain events, with virtually no integration. Rainwater samples were collected in 125mL glass bottles (bi-weekly samples) and 4mL glass vials (spot sampling), sealed with polyseal caps. Dripwater $\delta^{18}O$ samples were collected in 4mL glass vials with polyseal caps. Rainwater and dripwater $\delta^{18}O$ was measured using a GV Isoprime-Multiprep with a long-term reproducibility of ± 0.04‰ ($N > 500$), as calculated by repeat measurements of an internal water standard calibrated against NIST-VSMOW and NIST-GISP. All $\delta^{18}O$ data are reported with respect to VSMOW, unless otherwise stated.

A variety of climate datasets are used to provide an interpretive framework for the rainwater $\delta^{18}O$ variability. Daily rainfall at Gunung Mulu as measured at the Mulu airport is available since June, 1998 (data obtained from Sarawak Department of Irrigation and Drainage).

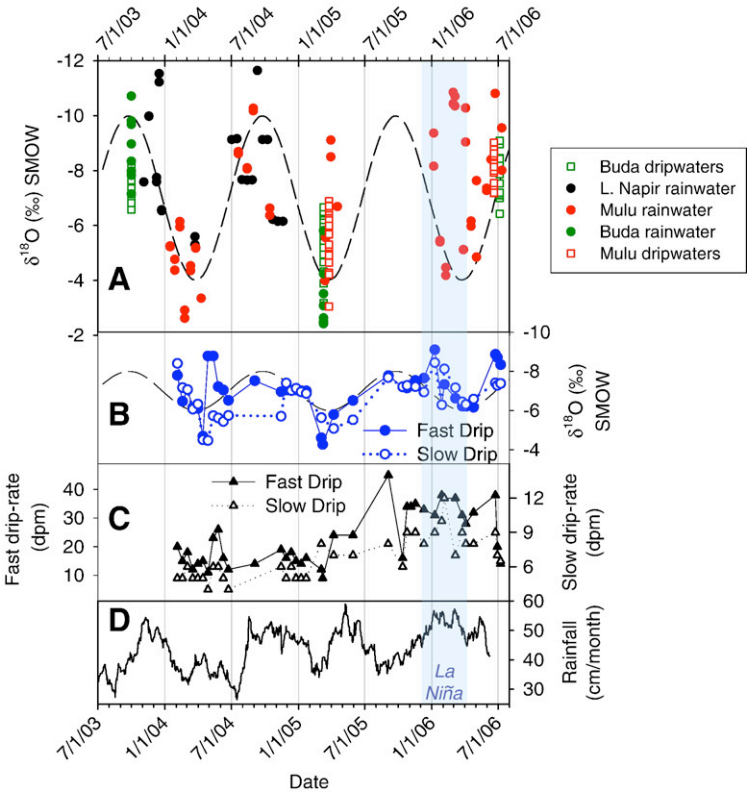

Fig. 6. Timeseries of rainwater, dripwater, and climate indices from October 2003 to July 2006. (A) Rainwater (circles) and dripwater (squares) $\delta^{18}O$ for Gunung Mulu (red) and Gunung Buda (green). Rainwater $\delta^{18}O$ data from nearby Long Napir (4°10′N, 115°8′E) are plotted in black circles. The dashed line represents an ad-hoc seasonal cycle in rainfall $\delta^{18}O$, based on a visual fit to the data. (B) Dripwater $\delta^{18}O$ timeseries for two drips located in Wind Cave, Gunung Mulu. The dashed line represents a low-amplitude version of the dashed line in panel A (same mean value and phase). (C) Drip-rate for timeseries drips plotted in (B). (D) Precipitation at Gunung Mulu airport, smoothed with a 3-month running average. The blue shaded vertical bar represents the time period associated with maximum precipitation anomalies during the 2005/2006 La Niña event.

Satellite-derived gridded precipitation data (CPC Merged Analysis of Precipitation; CMAP) (Xie and Arkin, 1997) are available since January, 1979 from the Climate Prediction Center. Daily rainfall data from the Global Precipitation Climatology Project (GPCP) data are available since January, 1997 from NASA (http://precip.gsfc.nasa.gov/). We rely on the shorter, local Mulu rainfall data for comparisons with the rainwater and dripwater isotopic data, and use the satellite-blended data to investigate large-scale precipitation variability over the Warm Pool. NCEP-NCAR reanalysis data (Kalnay et al., 1996) are used to obtain wind speed and direction since January, 1979, when high-quality CMAP precipitation data are available.

5. Results

5.1. Rainfall $\delta^{18}O$

The 3-yr timeseries of rainfall δ^{18}O in the vicinity of Gunung Mulu National Park covers intervals from October, 2003 to July, 2006 with variable resolution (Fig. 6A). Rainfall samples collected from three nearby stations (Gunung Buda, Gunung Mulu, and Long Napir) have similar δ^{18}O values, and are used interchangeably in analysis of the rainfall δ^{18}O timeseries. Rainfall δ^{18}O values range from − 11.5‰ to − 2.5‰, with a mean of − 6.7 ± 2.8‰ (1σ, $N = 97$). A ~ 6‰ seasonal cycle is visible, with lighter values (− 10‰) occurring from August to October and heavier values (− 4‰) occurring from December to March. Significant sub-seasonal rainfall δ^{18}O variability on the order of 4‰ is superimposed on the seasonal cycle, likely associated with synoptic variability (Treble et al., 2005a) that is poorly resolved with the bi-weekly rainfall sampling scheme.

The ~ 6‰ seasonal cycle in rainfall δ^{18}O cannot be ascribed to seasonality of precipitation amount, which has a weak semi-annual nature, with relative rainfall maxima occurring in late boreal spring and from September to December (Fig. 2). In fact, a low correlation between Mulu rainfall δ^{18}O and Mulu precipitation ($R = 0.05$) suggests a limited role for a local "amount effect" stemming from fractionation in a local convective event. Likewise, the observed seasonal variability cannot be explained by variations in source water δ^{18}O, which are less than 1‰ across the Warm Pool (Brown et al., 2006). Rather, we hypothesize that the observed rainfall δ^{18}O seasonality is caused by the increased rainout, and hence greater isotopic fractionation, that occurs during late boreal summer, and vice versa during late boreal winter. In late boreal summer, the ITCZ has reached its northern-most position, and mean southeasterly winds carry moisture from the Java Sea to Gunung Mulu, leading to significant rainout as moisture is carried long distances over the mountainous interior (Fig. 3). The remaining water vapor would be significantly depleted in δ^{18}O via both the "degree of rainout" and orographic fractionation mechanisms. Conversely, during late boreal winter, when the ITCZ lies south of Borneo, northeasterly winds carry moisture from the Sulu and South China Seas to Gunung Mulu (Fig. 3). The heavier rainfall δ^{18}O values measured during late boreal winter are consistent with the relatively short moisture pathway during this time of year.

Rainfall δ^{18}O values are relatively light from February to May 2006 (Fig. 6A), during the weak 2005/2006 La Niña event. Indeed, the 2005/2006 La Niña event represents the largest and most sustained SOI anomaly during the 3-yr monitoring program. Analysis of wind vectors and precipitation anomalies for the peak of the 2005/2006 La Niña reveals the canonical pattern of positive precipitation anomalies over most of the Warm Pool, including northern Borneo (Fig. 7).

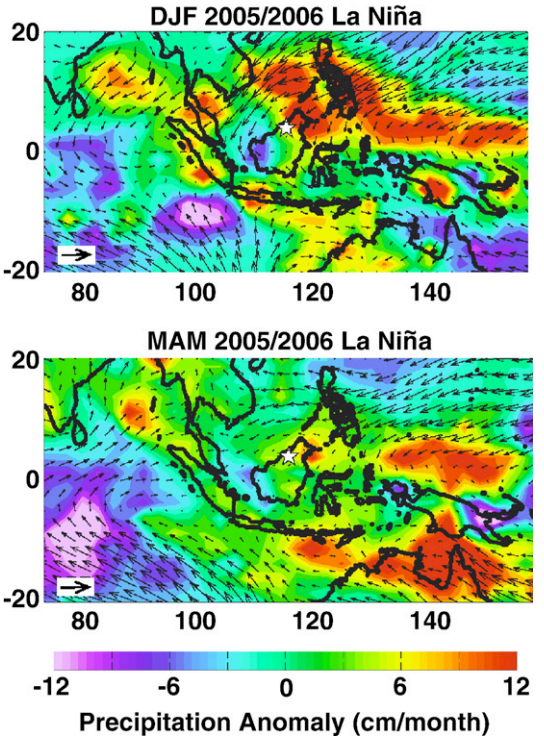

Fig. 7. Precipitation anomaly (colors) and wind vector (arrows) maps for the DJF (top) and MAM (bottom) periods during the weak 2005/2006 La Niña event. A 5 m/s wind vector (shown in white box) is plotted for reference.

Northeasterly winds in December–January–February and easterly winds in March–April–May likely advect moisture from areas characterized by enhanced precipitation to the east of Borneo (Fig. 7). This residual moisture would be isotopically depleted, having experienced significant rainout, and likely contributed to the depleted rainfall δ^{18}O values recorded at Gunung Mulu during this interval. Of course, enhanced precipitation at Gunung Mulu during the weak La Niña event could also result in depleted rainfall δ^{18}O. Therefore, the ENSO-related rainfall δ^{18}O signal is likely caused by a regional and/or local 'amount effect', whereby positive precipitation anomalies are associated with lighter rainfall δ^{18}O observed in northern Borneo during the 2005/2006 La Niña event.

Variable evapotranspiration rates may also affect the δ^{18}O of water vapor in northern Borneo, given that evapotranspiration contributes relatively enriched water vapor to the lower troposphere (Gat and Matsui, 1991) and plays an important role in the water balance in northern Borneo (Kumagai et al., 2005). Seasonal to interannual changes in evapotranspiration in Borneo are currently unconstrained, but such estimates may eventually come from analysis of satellite-derived measurements of the isotopic composition of tropospheric water vapor (e.g. Worden et al., 2007).

5.2. Dripwater $\delta^{18}O$

Dripwater δ^{18}O samples were collected every few weeks from two different drips located in Wind Cave at Gunung Mulu from February, 2004 to July, 2006. The so-called "fast drip" had a drip-rate of 10–45 drips per minute (dpm), falling from a 'shower-type' speleothem into a 'bathtub' rimmed with new calcite growth roughly 250m from the cave entrance. The "slow drip" fell at a rate of 4–12dpm from a small 2cm-long stalactite onto a mud bank, approximately 150m from the cave entrance. The mean δ^{18}O values for the fast and slow drips are indistinguishable (− 7.0 ± 1.1‰ and − 6.6 ± 1.0‰, respectively) and match the mean rainfall δ^{18}O value (− 6.7 ± 2.8‰) within error.

The fast and the slow drip δ^{18}O timeseries both exhibit seasonal variability on the order of 2–3‰ which tracks the rainfall δ^{18}O seasonal cycle (Fig. 6A and B). The fast drip δ^{18}O timeseries exhibits higher amplitude fluctuations than the slow drip, consistent with a shorter response time and/or less mixing in the overlying epikarst (Fig. 6B). The fact that sub-seasonal dripwater δ^{18}O variations of 1–2‰ are observed in the timeseries suggests that dripwater must move through the karst in less than 2months, although dripwater transit times likely vary with cumulative precipitation amount. The irregular temporal coverage of the dripwater δ^{18}O timeseries prevents the attribution of any given sub-seasonal δ^{18}O excursion to a specific precipitation event (Fig. 6D).

Large surveys of dripwater δ^{18}O conducted during the three field trips confirm that the seasonal variability and average value of the two timeseries drips in Wind Cave are broadly representative of drips throughout the Gunung Mulu and Gunung Buda caves (Fig. 8). The survey dripwater δ^{18}O values cluster in distinct δ^{18}O ranges depending on the timing of the fieldtrip with respect to the annual cycle of rainfall δ^{18}O. The average δ^{18}O value of the 150 spatial survey drips (characterized by drip-rates ranging from less than 0.1 to greater than 100dpm) is − 7.0 ± 1.0‰, in agreement with the average δ^{18}O of the timeseries drips (− 6.8 ± 1.1‰) and rainfall δ^{18}O (− 6.7 ± 2.8‰). The fact that the rainfall and dripwater δ^{18}O data scatter about the same average value means that minimal evaporation occurs between the ground surface and the dripwater site (which is not surprising given relative humidity values of ~ 100%).

Dripwater δ^{18}O values decrease during the 2005/2006 La Niña event, consistent with lower rainfall δ^{18}O observed during this period (Fig. 6B). Drip δ^{18}O values of − 8 to − 9‰ during January, 2006 are roughly 2‰ lighter than the previous year for both fast and slow drips, and remain low through March, with values as

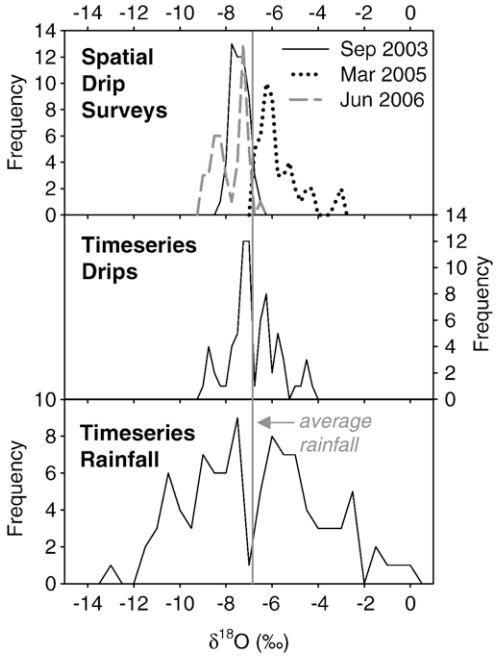

Fig. 8. Histograms of spatial dripwater, timeseries dripwater, and rainwater δ^{18}O values.

low as − 6‰ replacing more typical spring $\delta^{18}O$ values of − 4 to − 5‰. Unfortunately, there are no rainfall $\delta^{18}O$ samples for the period leading up to and including the peak dripwater $\delta^{18}O$ excursions in the first week of January, 2006, making it difficult to assess the relationship between the rainfall and dripwater $\delta^{18}O$ departures. While a more rigorous test of the ENSO-dripwater $\delta^{18}O$ relationship awaits the accumulation of data from multiple ENSO extremes over the next several years, the preliminary data from the 2005/2006 La Niña event strongly suggests that ENSO events are recorded as dripwater $\delta^{18}O$ anomalies at Gunung Mulu.

5.3. Drip-rate

The 3-yr drip-rate timeseries are characterized by significant monthly-scale variability that is superimposed on trends of increasing drip-rates through time. The slow and fast drip-rate timeseries are highly correlated (R = 0.67), implying that both drips are forced by the same history of karst recharge and discharge. Monthly-scale drip-rate variability bears little resemblance to the smoothed local precipitation timeseries, and may be governed by short-lived, extreme flushing events that are aliased in the bi-weekly drip-rate datasets (Perrin et al., 2003; Cruz et al., 2005a,b). On longer timescales, the 3-yr trends in both fast and slow drip-rates reflect a pronounced trend in precipitation at Gunung Mulu. The 2005/2006 La Niña period is characterized by maximum sustained drip-rates for both the fast and slow drips, indicative of a higher hydraulic head associated with anomalously high precipitation during this period. Therefore, even weak interannual variability has a profound impact on karst hydrology.

Weak but significant correlations exist between drip-rate and drip $\delta^{18}O$ for both the fast (R = 0.26) and slow (R = 0.37) drips, and reflect coherent responses to intraseasonal and interannual precipitation variability. However, the drip $\delta^{18}O$ timeseries do not exhibit the prominent trend observed in the drip-rate timeseries. Likewise, the drip-rate timeseries lack the seasonal variability observed in the dripwater $\delta^{18}O$ timeseries. In other words, dripwater $\delta^{18}O$ variability is controlled by rainwater $\delta^{18}O$ variability, which is only loosely tied to local precipitation amount on seasonal timescales. Drip-rate variability, on the other hand, appears to be directly related to local precipitation amount.

5.4. High-frequency variability in rainfall $\delta^{18}O$, dripwater $\delta^{18}O$, and drip-rate

High-frequency surveys conducted during the 2005 and 2006 fieldtrips reveal significant diurnal-to weekly-scale variability in rainwater $\delta^{18}O$, dripwater $\delta^{18}O$, and drip-rate (Fig. 9). Rainfall samples for this high-frequency

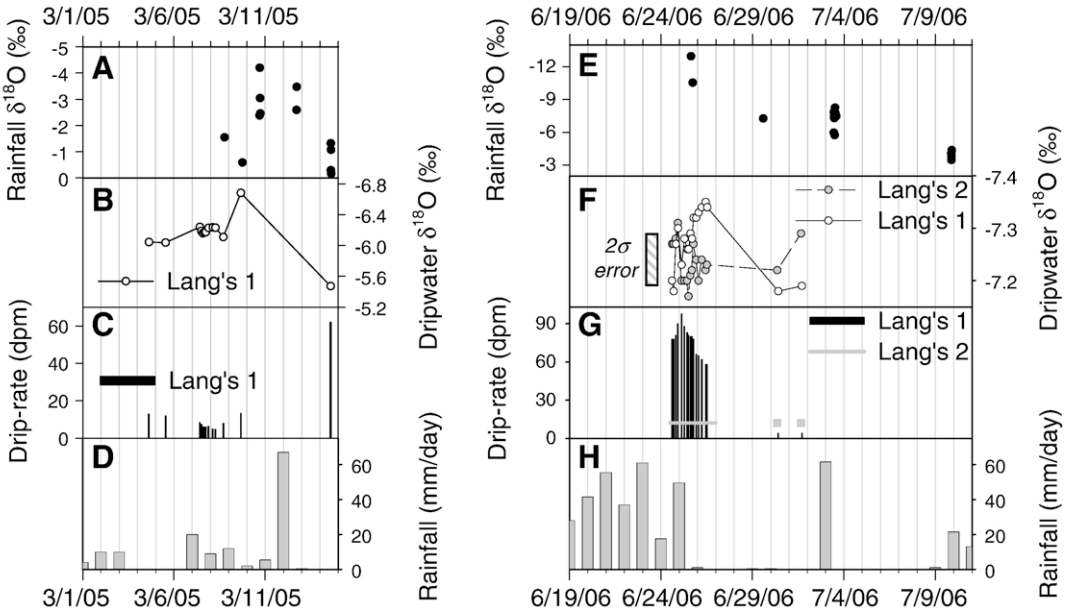

Fig. 9. High-resolution dripwater $\delta^{18}O$ and drip-rate timeseries for drips located in Lang's Cave, Gunung Mulu, plotted with daily precipitation values from Mulu aiport. (A–D) Results from the March 2005 fieldtrip. (E–H) Results from the June 2006 field trip. Note the expanded $\delta^{18}O$ scale in Panel F; the vertical hatched bar in Panel F represents the 2-sigma uncertainty for water $\delta^{18}O$ measurements at Georgia Tech.

study were collected in 4mL glass vials with polyseal tops, and as such represent virtually no time integration (in contrast to the rainfall $\delta^{18}O$ samples collected for the continuous timeseries discussed above, which represent rainfall integrated over a two-week period). It is important to note that on some days, rainfall samples were collected even though no rainfall was recorded at the Mulu airport, reflecting the patchiness of convective events in this area, especially during drier times. Dripwater samples were collected in Lang's Cave every few hours over the course of 1–2days to capture potential diurnal cycles, as well as once every few days during the fieldtrips' 2–3week duration to assess the impact of synoptic-scale variability.

Rainfall $\delta^{18}O$ values during both fieldtrips exhibit 2–3‰ variations in the course of a single day, and 8‰ variations over the course of several weeks (Fig. 9). Rainfall $\delta^{18}O$ during the March, 2005 fieldtrip ranges from − 4.2‰ to − 0.3‰, consistent with the seasonally high $\delta^{18}O$ values observed in the 3-yr rainfall $\delta^{18}O$ timeseries. Lighter rainfall $\delta^{18}O$ values (− 12‰ to − 3‰) measured during the June, 2006 fieldtrip are likewise consistent with seasonally isotopically depleted rainfall. Multiple samples collected over a period of several hours span from − 0.6‰ to − 4.2‰ for the 2005 fieldtrip and − 5.7‰ to − 8.3‰ for the 2006 fieldtrip (Fig. 9A and E, respectively).

Heavier rainfall $\delta^{18}O$ values likely represent more disorganized convection from vapor closer to equilibrium with seawater, while lighter values are indicative of condensation from a water vapor pool that has experienced significant distillation associated with prolonged, organized convection (Lawrence et al., 2004). Indeed, a rainfall $\delta^{18}O$ trend from − 12‰ on June 25, 2006 to − 4‰ on July 10, 2006 is associated with a marked decrease in precipitation — in the week leading up to June 25th, precipitation at Mulu airport averaged ~ 41mm/day, whereas in the two weeks leading up to July 10th, precipitation averaged ~ 4mm/day. The local precipitation change is linked to a large-scale shift in convective regime that occurred over the course of the 2006 fieldtrip, as observed in maps of precipitation and winds over the Maritime continent during this period (Fig. 10). Therefore, the well-organized, persistent, regional-scale convection that characterized the first days of the fieldtrip likely drove a strong depletion in water vapor $\delta^{18}O$, which when combined with lower evaporative enrichment associated with more humid lower atmospheric conditions, explains the depleted rainfall $\delta^{18}O$ values observed at Mulu. As this convective system moved eastwards in early July, depleted rainfall $\delta^{18}O$ gave way to unseasonably enriched rainfall $\delta^{18}O$ values, consistent with reduced rainout (less fractionation from a seawater source) and/or increased evaporative forcing as rain falls from a cloud. The speed and eastward propagation of the large-scale convective anomaly is consistent with intraseasonal climate variability (Madden and Julian, 1971; Madden and Julian, 1972; Knutson and Weickmann, 1987), which has a profound impact on Warm Pool precipitation, particularly during boreal summer (Hendon and Glick, 1997).

Dripwater $\delta^{18}O$ values measured during the March, 2005 and June, 2006 fieldtrips averaged − 6.15 ± 0.26‰ and − 7.25 ± 0.05‰, respectively, consistent with the seasonal cycle observed in the 3-yr dripwater $\delta^{18}O$ timeseries (Fig. 9B and F). Continuous bi-hourly sampling conducted over 24 h during the 2005 fieldtrip and over 48 h during the 2006 fieldtrip revealed no discernible diurnal cycle in dripwater $\delta^{18}O$ or drip-rate. There is no obvious relationship between rainfall $\delta^{18}O$ variability and dripwater $\delta^{18}O$ variability in either dataset, although there is appreciable day-to-day dripwater $\delta^{18}O$

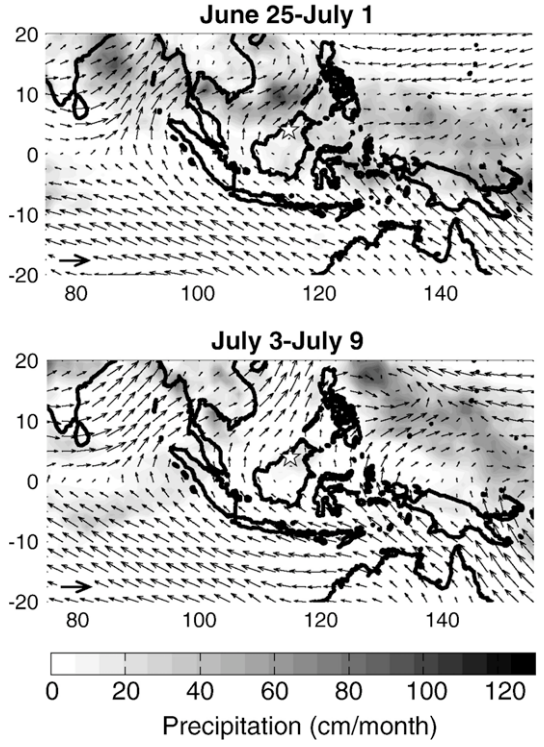

Fig. 10. (top) Map of precipitation and wind vectors averaged from June 25 through July 1, 2006. The analysis uses daily GPCP rainfall data available from http://precip.gsfc.nasa.gov/ and daily 1000 mb wind data from NCEP/NCAR reanalysis. A 5 m/s wind vector is plotted in the lower left-hand corner for reference. (bottom) Same as above but averaged from July 3 through July 9, 2006.

variability in the 2005 dataset. Heavy rains on March 12, 2005 trigger a flushing event (marked by drip-rates up to 60dpm) that may have led to the infiltration of rainfall with seasonally heavy $\delta^{18}O$ values, thereby explaining relatively heavy dripwater $\delta^{18}O$ values observed several days later. Oxygen isotopic variability of the same drip during the June, 2006 fieldtrip was much less pronounced, despite high-amplitude fluctuations in rainfall $\delta^{18}O$ and precipitation. The simultaneous monitoring of a second slower drip (Drip 2) located approximately 20m from the original drip (Drip 1) yielded results similar to Drip 1.

Day-to-day drip-rate variability for Drip 1 appears to be tied to rainfall amount, as drip-rate responds to large rainfall events in both 2005 and 2006. Drip 1 discharge peaks at 98dpm on June 25, 2006, immediately following a week of high precipitation, and falls to 4dpm after 10days of negligible rainfall. However, Drip 2′s drip-rate remains constant over the same time interval. The different responses of the two drips to the late June recharge event indicates that Drip 1 is likely fed in part by faster 'fissure flow', whereas Drip 2 represents slower 'seepage flow' whose response to hydraulic loading is significantly buffered (Ayalon et al., 1998). However, the $\delta^{18}O$ values for both Drip 1 and 2 remain relatively constant across the 2006 monitoring period, despite the introduction of relatively depleted rainfall $\delta^{18}O$ (− 11‰) to the epikarst during the late June recharge event. The stability of dripwater $\delta^{18}O$ during and after the late June recharge event implies a water residence time of greater than ~ 2weeks for the two Lang's Cave study drips.

The observation that drip-rate is more responsive to specific recharge events than dripwater $\delta^{18}O$ is not surprising, given that drip-rate is governed by instantaneous hydraulic pressure changes in the water flow pathway (Genty and Deflandre, 1998; Baker and Brunsdon, 2003; Sondag et al., 2003), while dripwater composition reflects a cumulative mixture of past rainfall events (Ayalon et al., 1998; Perrin et al., 2003; Cruz et al., 2005a,b).

6. Discussion

6.1. Comparison with isotope AGCMs

Atmospheric general circulation models (AGCMs) equipped with isotope trace modules are valuable tools for assessing the relationship between large-scale climate and rainfall $\delta^{18}O$ (Jouzel et al., 1987; Hoffmann et al., 1998; Cole et al., 1999; Noone and Simmonds, 2002; Vuille et al., 2005; Brown et al., 2006). Large-scale precipitation patterns are generally well-represented in the AGCMs, although the largest deficiencies occur in tropical zones characterized by deep convection. Therefore, it is useful to compare the isotope AGCM output for northern Borneo with the rainfall $\delta^{18}O$ timeseries collected at Gunung Mulu, which represents the only available rainfall $\delta^{18}O$ timeseries in a 1000km radius. The observed annual mean weighted rainfall $\delta^{18}O$ value at Gunung Mulu (− 6.8‰) agrees moderately well with modeled annual mean weighted rainfall $\delta^{18}O$ values for northern Borneo, which range from − 6‰ in a high-resolution version of ECHAM-4 (Vuille et al., 2005) to − 8‰ in a low-resolution version of NASA-GISS (Cole et al., 1999). Such depleted rainwater $\delta^{18}O$ values are characteristic of zones of deep convection, where high levels of rainout lead to effective distillation of the water vapor pool. The prominent 6‰ seasonal cycle of rainfall $\delta^{18}O$ observed at Gunung Mulu is not well-reproduced in model results, however, which show seasonal cycles of 1–2‰ in northern Borneo (Vuille et al., 2005; Brown et al., 2006). This discrepancy may derive from an over-dependence of rainfall $\delta^{18}O$ on local precipitation amount in the AGCMs, and/or deficiencies associated with the models' coarse resolutions, which do not adequately resolve marginal seas nor the high topography in central Borneo.

Interannual rainfall $\delta^{18}O$ variability is difficult to quantify in the 3-yr Gunung Mulu timeseries, but increased precipitation during the weak 2005/2006 La Niña event caused a > 2‰ depletion in rainfall $\delta^{18}O$. Models demonstrate a high sensitivity of West Pacific rainfall $\delta^{18}O$ to ENSO variability, whereby increased rainfall during a La Niña event leads to depleted rainfall $\delta^{18}O$ via the amount effect (Hoffmann et al., 1998; Cole et al., 1999; Vuille et al., 2005; Brown et al., 2006) but the magnitude of the interannual $\delta^{18}O$ anomalies are model-dependent. While the models provide a useful framework for assessing large-scale features of the climate-rainfall $\delta^{18}O$ relationship in the tropics, local processes such as topographically-driven precipitation, variable moisture trajectories, and even evapotranspiration likely contribute to the observed rainfall $\delta^{18}O$ variability at Gunung Mulu. More realistic simulations of rainfall $\delta^{18}O$ over the Maritime continent likely require nesting a high-resolution isotope AGCM with realistic topography, coastlines, and land-atmosphere coupling within a coarser-resolution AGCM of the type studied thus far.

6.2. Implications for stalagmite $\delta^{18}O$ reconstructions

The utility of stalagmite $\delta^{18}O$ reconstructions of paleoclimate depends on firm knowledge of the relationship

between climate and rainfall $\delta^{18}O$, and how rainfall $\delta^{18}O$ signals are manifest in dripwater $\delta^{18}O$ variability. In northern Borneo, rainfall $\delta^{18}O$ is controlled by moisture trajectory (which varies seasonally but not interannually) and precipitation amount (which varies appreciably on intraseasonal and interannual timescales but does not vary seasonally). Both of these mechanisms involve Raleigh distillation processes, whether via regional 'degree of rainout' and/or more local 'amount' effects (Dansgaard, 1964; Rozanski et al., 1993; Gat, 1996). A new daily rainfall sampling program at Gunung Mulu, when combined with meteorological data from a newly-installed weather station, should further resolve the relationship between large-scale climate, local climate, and local rainfall $\delta^{18}O$ on synoptic to interannual timescales.

The dripwater $\delta^{18}O$ data demonstrate that for moderately fast drips (4–20dpm), dripwater $\delta^{18}O$ variability represents a damped response to rainfall $\delta^{18}O$ variability averaged over approximately 2–3months. The average $\delta^{18}O$ value of rainwaters (-6.7 ± 2.8‰), slow dripwaters (-6.6 ± 1.0‰), and fast dripwaters (-7.0 ± 1.1‰) agree within error, bolstering confidence in the interpretation of stalagmite $\delta^{18}O$ records as rainfall $\delta^{18}O$ reconstructions, assuming equilibrium calcite precipitation. For the Gunung Buda stalagmites analyzed so far, modern calcite $\delta^{18}O$ is approximately -9.1‰ PDB (Partin et al., 2007), in good agreement with calculated calcite $\delta^{18}O$ values in equilibrium with dripwaters at -6.8‰SMOW and temperatures of 26°C (Kim and O'Neil, 1997). However, stalagmites from other tropical sites are associated with significant isotopic disequilibrium effects (Mickler et al., 2004).

Fast-growing stalagmites may record the seasonal cycle in rainfall $\delta^{18}O$ (Treble et al., 2005b; Johnson et al., 2006), while slow-growing stalagmites would record changes in the annual average of rainfall $\delta^{18}O$. Changes in the strength and/or location of the ITCZ could alter annual average rainfall $\delta^{18}O$ by shifting the balance of seasonal rainfall $\delta^{18}O$ extremes (currently more negative in boreal summer and more positive in boreal winter). Given the skewed nature of ENSO variability (more low-amplitude La Niña events separated by fewer high-amplitude El Niño events (Burgers and Stephenson, 1999)), a change in the intensity of ENSO variability would impart a signal on long-term mean rainfall $\delta^{18}O$. By analogy to the observed response of the climate-karst system to ENSO variability, heavier stalagmite $\delta^{18}O$ values in the Gunung Mulu/Buda stalagmite $\delta^{18}O$ records reflect a reduction in deep convection in the vicinity of Borneo, indicative of relatively dry conditions.

7. Conclusions

Taken together, the present study confirms that seasonal to interannual changes in large-scale precipitation are reflected in both rainwater and dripwater $\delta^{18}O$ variability in northern Borneo. Borneo is the largest landmass in the Maritime Continent, and seasonal changes in surface wind direction associated with the north-to-south migration of the ITCZ drive large seasonal changes in rainfall $\delta^{18}O$ that are recorded in muted seasonal cycles of dripwater $\delta^{18}O$. Rainwater and dripwater $\delta^{18}O$ values are lightest during late boreal summer, and heaviest during late boreal winter. Interannual rainfall and dripwater $\delta^{18}O$ anomalies at Gunung Mulu are linked to regional-scale changes in convective activity associated with ENSO variability, whereby increased precipitation drives more negative rainfall and dripwater $\delta^{18}O$, consistent with the 'amount effect'. An 8‰ change in rainfall $\delta^{18}O$ over the course of two weeks dwarfs seasonal to interannual rainfall $\delta^{18}O$ changes, and highlights the importance of large-scale (1000km) climatic controls on rainfall $\delta^{18}O$ in northern Borneo. Whereas dripwater $\delta^{18}O$ is buffered against high-frequency (synoptic and intraseasonal-scale) variability observed in rainfall $\delta^{18}O$, drip-rate exhibits a faster response time, likely driven by changes in hydraulic loading. On longer timescales, drip-rate is correlated to cumulative precipitation over the previous several months, and resembles a 6-month smoothed version of local precipitation. Stalagmite $\delta^{18}O$ records from Gunung Mulu likely reflect changes in the strength and/or position of the ITCZ combined with changes in the amplitude and/or frequency of ENSO extremes, whereby heavier $\delta^{18}O$ is indicative of relatively dry conditions. More generally, this study demonstrates how site-specific studies of the climate-rainfall $\delta^{18}O$ relationship can improve the paleoclimatic interpretations of rainfall $\delta^{18}O$ reconstructions from geologic archives such as ice cores, tree rings, and lake sediments.

Acknowledgements

The authors are indebted to Jenny Malang and the staff of Gunung Mulu National Park for fieldtrip and sampling assistance, Johnny Baei Hassan for expert caving guidance, and Prof. Andrew Tuen (UNIMAS) for permitting assistance. Joel Despain, George Prest, Shane Fryer, Jed Mosenfelder, and Brad Hacker provided assistance during the 2003 fieldtrip. Permits for this work were granted by the Malaysian Economic Planning Unit, the Sarawak Forestry Department, and the Sarawak State Planning Unit. Mulu airport rainfall

was provided by the Sarawak Department of Irrigation and Drainage. The research was funded by NSF grant ATM-0318445, and by a Comer Abrupt Climate Change Fellowship.

References

Araguas-Araguas, L., Froehlich, K., Rozanski, K., 1998. Stable isotope composition of precipitation over southeast Asia. J. Geophys. Res. Atmos. 103, 28721–28742.

Ayalon, A., Bar-Matthews, M., Sass, E., 1998. Rainfall-recharge relationships within a karstic terrain in the eastern Mediterranean semi-arid region, Israel: delta O-18 and delta D characteristics. J. Hydrol. 207, 18–31.

Baker, A., Brunsdon, C., 2003. Non-linearities in drip water hydrology: an example from Stump Cross Caverns, Yorkshire. J. Hydrol. 277, 151–163.

Bar-Matthews, M., Ayalon, A., Kaufman, A., Wasserburg, G.J., 1999. The Eastern Mediterranean paleoclimate as a reflection of regional events: Soreq cave, Israel. Earth Planet. Sci. Lett. 166, 85–95.

Brown, J., Simmonds, I., Noone, D., 2006. Modeling delta O-18 in tropical precipitation and the surface ocean for present-day climate. J. Geophys. Res. Atmos. 111, D05105.

Burgers, G., Stephenson, D.B., 1999. The "normality" of El Nino. Geophys. Res. Lett. 26, 1027–1030.

Burns, S.J., Fleitmann, D., Mudelsee, M., Neff, U., Matter, A., Mangini, A., 2002. A 780-year annually resolved record of Indian Ocean monsoon precipitation from a speleothem from south Oman. J. Geophys. Res. Atmos. 107.

Burns, S.J., Fleitmann, D., Matter, A., Kramers, J., Al-Subbary, A.A., 2003. Indian Ocean climate and an absolute chronology over Dansgaard/Oeschger events 9 to 13. Science 301, 1365–1367.

Cole, J.E., Rind, D., Webb, R.S., Jouzel, J., Healy, R., 1999. Climatic controls on interannual variability of precipitation delta O-18: simulated influence of temperature, precipitation amount, and vapor source region. J. Geophys. Res. Atmos. 104, 14223–14235.

Cruz, F.W., Burns, S.J., Karmann, I., Sharp, W.D., Vuille, M., Cardoso, A.O., Ferrari, J.A., Dias, P.L.S., Viana, O., 2005a. Insolation-driven changes in atmospheric circulation over the past 116,000 years in subtropical Brazil. Nature 434, 63–66.

Cruz, F.W., Karmann, I., Viana, O., Burns, S.J., Ferrari, J.A., Vuille, M., Sial, A.N., Moreira, M.Z., 2005b. Stable isotope study of cave percolation waters in subtropical Brazil: Implications for paleoclimate inferences from speleothems. Chem. Geol. 220, 245–262.

Cruz, F.W., Burns, S.J., Karmann, I., Sharp, W.D., Vuille, M., 2006. Reconstruction of regional atmospheric circulation features during the late Pleistocene in subtropical Brazil from oxygen isotope composition of speleothems. Earth Planet. Sci. Lett. 248, 495–507.

Dansgaard, W., 1964. Stable isotopes in precipitation. Tellus 16, 436–468.

Dykoski, C.A., Edwards, R.L., Cheng, H., Yuan, D.X., Cai, Y.J., Zhang, M.L., Lin, Y.S., Qing, J.M., An, Z.S., Revenaugh, J., 2005. A high-resolution, absolute-dated Holocene and deglacial Asian monsoon record from Dongge Cave, China. Earth Planet. Sci. Lett. 233, 71–86.

Fleitmann, D., Burns, S.J., Mudelsee, M., Neff, U., Kramers, J., Mangini, A., Matter, A., 2003. Holocene forcing of the Indian monsoon recorded in a stalagmite from Southern Oman. Science 300, 1737–1739.

Fleitmann, D., Burns, S.J., Neff, U., Mudelsee, M., Mangini, A., Matter, A., 2004. Palaeoclimatic interpretation of high-resolution oxygen isotope profiles derived from annually laminated speleothems from Southern Oman. Quat. Sci. Rev. 23, 935–945.

Friedman, I., Smith, G.I., Gleason, J.D., Warden, A., Harris, J.M., 1992. Stable isotope composition of waters in Southeastern California. 1. Modern precipitation. J. Geophys. Res. Atmos. 97, 5795–5812.

Gat, J.R., 1996. Oxygen and hydrogen isotopes in the hydrologic cycle. Annual Rev. Earth Platet. Sci. 24, 225–262.

Gat, J.R., Matsui, E., 1991. Atmospheric water-balance in the Amazon Basin — an isotopic evapotranspiration Model. J. Geophys. Res. Atmos. 96, 13179–13188.

Genty, D., Deflandre, G., 1998. Drip flow variations under a stalactite of the Pere Noel cave (Belgium). Evidence of seasonal variations and air pressure constraints. J. Hydrol. 211, 208–232.

Grootes, P.M., Stuiver, M., White, J.W.C., Johnsen, S., Jouzel, J., 1993. Comparison of oxygen-isotope records from the GISP2 and GRIP Greenland Ice cores. Nature 366, 552–554.

Hazebroeck, H.P., Morshidi, A.K.A., 2002. A Guide to Gunung Mulu National Park, Natural History Publications (Borneo), Kota Kinabalu, 91 pp.

Hendon, H.H., Glick, J., 1997. Intraseasonal air-sea interaction in the tropical Indian and Pacific Oceans. J. Climate 10, 647–661.

Hoffmann, G., Werner, M., Heimann, M., 1998. Water isotope module of the ECHAM atmospheric general circulation model: a study on timescales from days to several years. J. Geophys. Res. Atmos. 103, 16871–16896.

Johnson, K.R., Hu, C.Y., Belshaw, N.S., Henderson, G.M., 2006. Seasonal trace-element and stable-isotope variations in a Chinese speleothem: the potential for high-resolution paleomonsoon reconstruction. Earth Planet. Sci. Lett. 244, 394–407.

Jouzel, J., Russell, G.L., Suozzo, R.J., Koster, R.D., White, J.W.C., Broecker, W.S., 1987. Simulations of the HDO and H2 O-18 atmospheric cycles using the NASA GISS general-circulation model — the seasonal cycle for present-day conditions. J. Geophys. Res. Atmos. 92, 14739–14760.

Kalnay, E., Kanamitsu, M., Kistler, R., Collins, W., Deaven, D., Gandin, L., Iredell, M., Saha, S., White, G., Woollen, J., Zhu, Y., Chelliah, M., Ebisuzaki, W., Higgins, W., Janowiak, J., Mo, K.C., Ropelewski, C., Wang, J., Leetmaa, A., Reynolds, R., Jenne, R., Joseph, D., 1996. The NCEP/NCAR 40-year reanalysis project. Bull. Am. Meteorol. Soc. 77, 437–471.

Kim, S.-T., O'Neil, J.R., 1997. Equilibrium and non-equilibrium oxygen isotope effects in synthetic carbonates. Geochim. Cosmochim. Acta 61, 3461–3475.

Knutson, T.R., Weickmann, K.M., 1987. 30–60day atmospheric oscillations — composite life-cycles of convection and circulation anomalies. Mon. Weather Rev. 115, 1407–1436.

Kumagai, T., Saitoh, T.M., Sato, Y., Takahashi, H., Manfroi, O.J., Morooka, T., Kuraji, K., Suzuki, M., Yasunari, T., Komatsu, H., 2005. Annual water balance and seasonality of evapotranspiration in a Bornean tropical rainforest. Agric. For. Meteorol. 128, 81–92.

Lachniet, M.S., Burns, S.J., Piperno, D.R., Asmerom, Y., Polyak, V.J., Moy, C.M., Christenson, K., 2004. A 1500-year El Nino/Southern Oscillation and rainfall history for the Isthmus of Panama from speleothem calcite. J. Geophys. Res. Atmos. 109.

Lau, N.C., Nath, M.J., 2000. Impact of ENSO on the variability of the Asian–Australian monsoons as simulated in GCM experiments. J. Climate 13, 4287–4309.

Lau, N.C., Nath, M.J., 2003. Atmosphere-ocean variations in the Indo–Pacific sector during ENSO episodes. J. Climate 16, 3–20.

Lawrence, J.R., Gedzelman, S.D., Dexheimer, D., Cho, H.K., Carrie, G.D., Gasparini, R., Anderson, C.R., Bowman, K.P., Biggerstaff,

M.I., 2004. Stable isotopic composition of water vapor in the tropics. J. Geophys. Res. Atmos. 109, D06115.
Madden, R.A., Julian, P.R., 1971. Detection of a 40–50day oscillation in zonal wind in tropical pacific. J. Atmos. Sci. 28, 702–708.
Madden, R.A., Julian, P.R., 1972. Description of global-scale circulation cells in tropics with a 40–50day period. J. Atmos. Sci. 29, 1109–1123.
McDonald, J., Drysdale, R., Hill, D., 2004. The 2002–2003 El Nino recorded in Australian cave drip waters: implications for reconstructing rainfall histories using stalagmites. Geophys. Res. Lett. 31, L22202.
Mickler, P.J., Banner, J.L., Stern, L., Asmerom, Y., Edwards, R.L., Ito, E., 2004. Stable isotope variations in modern tropical speleothems: evaluating equilibrium vs. kinetic isotope effects. Geochim. Cosmochim. Acta 68, 4381–4393.
Noone, D., Simmonds, I., 2002. Associations between delta O-18 of water and climate parameters in a simulation of atmospheric circulation for 1979–95. J. Climate 15, 3150–3169.
Partin, J.W., Cobb, K.M., Adkins, J.F., Fernandez, D.P., Clark, B., 2007. Millennial-scale trends in West Pacific Warm Pool hydrology from the Last Glacial Maximum to present, Nature 499, 452–455. doi:10.1038/nature06164.
Perrin, K., Jeannin, P.Y., Zwahlen, F., 2003. Epikarst storage in a karst aquifer: a conceptual model based on isotopic data, Milandre test site, Switzerland. J. Hydrol. 279, 106–124.
Rasmusson, E.M., Wallace, J.M., 1983. Meteorlogical aspects of the El Niño/Southern Oscillation. Science 222, 1195–1202.
Ropelewski, C.F., Halpert, M.S., 1987. Global and regional scale precipitation patterns associated with the El Nino/Southern Oscillation. Mon. Weather Rev. 115, 1606–1626.
Rozanski, K., Araguas-Araguas, L., Gonfiantini, R., 1993. Isotopic patterns in modern global precipitation. In: Swart, P.K., Lohmann, K.C., McKenzie, J. (Eds.), Climate Change in Continental Isotopic Records. Geophysical Monograph, vol. 78. American Geophysical Union, Washington D.C., pp. 1–36.
Siegenthaler, U., Oeschger, H., 1980. Correlation of 18O in precipitation with temperature and altitude. Nature 285, 314–417.
Sondag, F., van Ruymbeke, M., Soubies, F., Santos, R., Somerhausen, A., Seidel, A., Boggiani, P., 2003. Monitoring present day climatic conditions in tropical caves using an Environmental Data Acquisition System (EDAS). J. Hydrol. 273, 103–118.
Treble, P.C., Budd, W.F., Hope, P.K., Rustomji, P.K., 2005a. Synoptic-scale climate patterns associated with rainfall delta O-18 in southern Australia. J. Hydrol. 302, 270–282.
Treble, P.C., Chappell, J., Gagan, M.K., McKeegan, K.D., Harrison, T.M., 2005b. In situ measurement of seasonal delta O-18 variations and analysis of isotopic trends in a modem speleothem from southwest Australia. Earth Planet. Sci. Lett. 233, 17–32.
Vuille, M., Werner, M., 2005. Stable isotopes in precipitation recording South American summer monsoon and ENSO variability: observations and model results. Clim. Dyn. 25, 410–413.
Vuille, M., Werner, M., Bradley, R.S., Keimig, F., 2005. Stable isotopes in precipitation in the Asian monsoon region. J. Geophys. Res. Atmos. 110, D23108.
Wang, Y.J., Cheng, H., Edwards, R.L., An, Z.S., Wu, J.Y., Shen, C.C., Dorale, J.A., 2001. A high-resolution absolute-dated Late Pleistocene monsoon record from Hulu Cave, China. Science 294, 2345–2348.
Wang, X., Auler, A.S., Edwards, R.L., Cheng, H., Ito, E., Solheid, M., 2006. Interhemispheric anti-phasing of rainfall during the last glacial period. Quat. Sci. Rev. 25, 3391–3403.
Worden, J., Noone, D., Bowman, K., 2007. Importance of rain evaporation and continental convection in the tropical water cycle. Nature 445, 528–532.
Xie, P.P., Arkin, P.A., 1997. Global precipitation: a 17-year monthly analysis based on gauge observations, satellite estimates, and numerical model outputs. Bull. Am. Meteorol. Soc. 78, 2539–2558.
Yuan, D.X., Cheng, H., Edwards, R.L., Dykoski, C.A., Kelly, M.J., Zhang, M.L., Qing, J.M., Lin, Y.S., Wang, Y.J., Wu, J.Y., Dorale, J.A., An, Z.S., Cai, Y.J., 2004. Timing, duration, and transitions of the Last Interglacial Asian Monsoon. Science 304, 575–578.